Chemistry & Biology
Article

Incomplete β-Ketone Processing as a Mechanism for Polyene Structural Variation in the FR-008/Candicidin Complex

Yongjun Zhou,[1] Jialiang Li,[1] Jing Zhu,[2] Shi Chen,[1] Linquan Bai,[1] Xiufen Zhou,[1] Houming Wu,[2,*] and Zixin Deng[1,*]
[1]Laboratory of Microbial Metabolism and School of Life Science & Biotechnology, Shanghai Jiaotong University, Shanghai 200030, China
[2]State Key Laboratory of Bio-Organic and Natural Products Chemistry, Shanghai Institute of Organic Chemistry, Chinese Academy of Sciences, Shanghai 200032, China
*Correspondence: zxdeng@sjtu.edu.cn (Z.D.), hmwu@mail.sioc.ac.cn (H.W.)
DOI 10.1016/j.chembiol.2008.05.007

SUMMARY

FR-008/candicidin is a heptaene macrolide with established antifungal activity, produced by *Streptomyces* sp. FR-008 as a complex mixture of compounds. Here, six components (FR-008-I to -VI) of the FR-008/candicidin complex were determined; III, V, and VI were confirmed as natural products, principally differing from each other at C-3 and C-9, while the other three were believed to originate from the respective conversions of the natural ones in vitro. Inactivation of KR21 and DH18, respectively, abolished production of V carrying a C-3 hydroxyl, and VI carrying a C-9 methylene. Combined inactivation created a mutant producing only III, with a C-3 ketone and a C-9 hydroxyl, and having antifungal activity superior to V and comparable to VI. Incomplete activities of KR21 and DH18 were, therefore, unambiguously identified as being involved in structural variations of FR-008 complex.

INTRODUCTION

Antifungal polyene macrolides, synthesized mainly by bacteria, are a large class of natural products consisting of 20 to 44 membered macrolactone rings with a characteristic series of three to eight conjugated double bonds, as well as an exocyclic carboxyl group and an unusual mycosamine sugar (Aparicio et al., 2003). The academically and therapeutically relevant examples are four glycosylated polyenes, amphotericin, pimaricin, nystatin, and FR-008/candicidin, of which the biosynthetic gene clusters have been sequenced and well analyzed as a class of so-called type I modular polyketide synthases (PKSs) (Aparicio et al., 2000; Brautaset et al., 2000; Caffrey et al., 2001; Campelo and Gil, 2002; Chen et al., 2003).

Aside from being well known as effective clinical antifungal agents, some glycosylated polyenes also inhibit HIV replication, hamper the development of prion-related diseases, and can even be useful in cancer therapies (Zotchev, 2003). Mechanistically, polyene macrolides generally interact with ergosterol in the fungal cell membrane, causing leakage of small molecules and ions, and resulting in cell death (Bolard, 1986). However, their affinity for cholesterol in the mammalian cell membrane causes polyene macrolides to have serious side effects (Zotchev, 2003). Moreover, water insolubility general displayed by polyene macrolides also limits their clinical application. There is, thus, an urgent need to develop novel polyene derivatives with improved pharmacological properties, or with reduced side effects.

Type I polyketide biosynthesis is catalyzed by modular PKSs that usually consist of giant multifunctional proteins with discrete catalytic domains responsible for each successive cycle in chain building and modification (Hopwood and Sherman, 1990; Katz and Donadio, 1993). Each set, or module, of domains is responsible for one cycle of polyketide chain elongation, and minimally consists of three functional domains: ketosynthase (KS), acyltransferase (AT), and acyl carrier protein (ACP). Besides, PKS module may optionally contain modifying domains (i.e., a ketoreductase [KR], a dehydratase [DH], and/or an enoyl reductase [ER]). The KR reduces the β-ketothioester intermediate generated by the KS to a β-hydroxythioester, and the DH dehydrates the resulting intermediate into an α,β-unsaturated ester, while the ER hydrogenates the olefin to yield a fully reduced β-carbon atom (Schwecke et al., 1995). Post-PKS steps, such as sugar attachment, hydroxylation, and methylation, further diversify the structures of the end-products.

The complexities of PKS pathways result in their metabolites usually being produced as a series of structurally related components by variation of either the PKS or post-PKS steps. Many structurally related derivatives of polyketides have been attributed to variations during chain assembly, including the generation of keto, hydroxyl, enoyl, or methylene groups in the carbon chain by variations in KR, DH, and ER activity. Substrate flexibility of the AT in the loading domain creates a series of avermectin derivatives, and epothilones A and B were presumed to be coproduced by the relaxed specificity of AT4 accepting either malonyl or methylmalonyl extender units (Ikeda et al., 1999; Marsden et al., 1998; Tang et al., 2000). Pikromycin macrolactones were coproduced as 12 and 14 membered rings by "skipping" of the final condensation cycle (Xue and Sherman, 2000). Incomplete DH2 activity in avermectin biosynthesis resulted in two groups of compounds containing a hydroxyl group or enoyl carbons at C22-23 (Ikeda et al., 1999). Sluggish ER5 in AmphC should account for the coexistence of amphotericins A and B (Caffrey et al., 2001), and failed enoyl reduction (ER5) was proposed to give several heptaene nystatin derivatives (Bruheim et al., 2004). Post-PKS variations include the production of

erythromycin A and B as a result of incomplete C-12 hydroxylation by EryK (Stassi et al., 1998), and nystatin A_1, A_3, and NYST1070 are generated by different sugar moiety attachment (Bruheim et al., 2004).

Manipulation of such variation can be exploited to produce more useful products or reduce undesired byproduct levels. The production of a desired avermectin derivative (CHC-B2) was improved by engineering the *aveC* gene to improve the efficacy of DH2 in AVES1 (Stutzman-Engwall et al., 2005). Mutagenesis of *eryF* and *eryK*, respectively encoding C-6 and C-12 hydroxylations in erythromycin, accelerated the accumulation of 6,12-dideoxyerythromycin A (Stassi et al., 1998).

FR-008/candicidin, a heptaene macrolide with antifungal activity, is produced by *Streptomyces* sp. FR-008. Bioinformatic and mutational analysis of the completely sequenced FR-008 gene cluster revealed FR-008 to be synthesized by a typical type I PKS pathway composed of 21 elongation steps and two late modifications (i.e., carboxylation and mycosamine attachment) (Chen et al., 2003; Hu et al., 1994). Four structurally related compounds, FR-008-I to -IV (named FR-008 series to distinguish them from the identical compounds, candicidin A to D, produced by *Streptomyces griseus* IMRU3570; Campelo and Gil, 2002; Zielinski et al., 1979), were believed to constitute the FR-008 mixture, of which FR-008-II was confirmed by NMR and considered as an isomer of FR-008-III due to equivalence of hemiketal moiety formation between C-15 and C-19 on the FR-008 aglycone in vitro (Chen et al., 2003).

Here we describe improved LC-MS analysis of FR-008 complex and NMR characterization of three main FR-008 components. Initially, six components (FR-008-I to -VI), instead of four previously detected from *Streptomyces* sp. FR-008 and *S. griseus* IMRU3570, were examined for their exact chemical structures. FR-008-V, -III, and -VI, were compared with previously reported FR-008-I, -II, and -IV, respectively, of which the isomeric relationship of II and III was further confirmed by NMR analysis in our work. Combined with the structural information, further point-mutation experiments proved that the coproduction of the three FR-008 compounds (FR-008-III, -V, and -VI) was principally induced by incomplete activities of KR21 and DH18 during polyketide chain elongation. Notably, double mutagenesis of KR21 and DH18 created a novel strain, producing only FR-008-III with an antifungal activity superior to that of FR-008-V and comparable to that of FR-008-VI. The results establish that domain modification (e.g., DH, KR, or ER) in a PKS can be manipulated effectively to generate structural variations and/or for rational accumulation of a pure metabolite with superior activity.

RESULTS

Structural Elucidation of FR-008 Compounds

The FR-008 complex was reported to consist of four main components, FR-008-I, -II, -III, and -IV, in vivo, of which FR-008-II was confirmed by NMR and assumed to be an isomer of FR-008-III due to equilibrium of hemiketal moiety formation between C-15 and C-19 on the FR-008 aglycone (Chen et al., 2003). A reexamination of the FR-008 extract from liquid fermentation broth by improved LC/ESI-MS analysis, however, indicated coexistence of six components instead of four (Figure 1A). They can be grouped as three pairs of isomers (instead of one) by their identical MS spectra (i.e., the pairs FR-008-I and -V [$(M - H)^-$ = 1110.6; $(M + H)^+$ = 1112.1], FR-008-II and -III [$(M - H)^-$ = 1108.8; $(M + H)^+$ = 1110.0], and FR-008-IV and -VI [$(M - H)^-$ = 1092.9; $(M + H)^+$ = 1094.0]. In freshly made extracts of mycelia from liquid fermentation or spores from solid fermentation, in contrast, only FR-008-V, -III, and -VI could be detected, and their isomers (FR-008-I, -II, and -IV) only appeared later, after the samples were kept at room temperature for 1 or more days (Figure 1B), implying that only FR-008-III, -V, and -VI are authentic natural products of FR-008 biosynthesis.

FR-008-III, -V, and -VI were purified by preparative reverse-phase HPLC and subjected to LC/ESI-MS and NMR (600 MHz, DMSO-d_6) analyses. Their structures were determined by 1D and 2D-NMR spectroscopy, including double quantum filter correlated spectroscopy (DQF-COSY), total correlated spectroscopy (TOCSY), nuclear Overhauser enhancement spectroscopy, heteronuclear multiple quantum coherence and heteronuclear multiple bond correlation. According to NMR data, FR-008-III was confirmed as being identical to candicidin D (Zielinski et al., 1979). In contrast to the documented FR-008-II (Chen et al., 2003), FR-008-III, -V, and -VI all have a hemiketal moiety between C-15 and C-19 with the quaternary carbon signals located between δ96.4 and δ97.4 on their ^{13}C-NMR spectra (see the Supplemental Data available online).

The difference between FR-008-V and -III is only at C-3, where a hydroxyl group present in the former is replaced by a keto-group in the latter (Figure 1B). Comparison of ^{13}C-NMR and ^{1}H-NMR data of FR-008-V with those of FR-008-III revealed lack of carbonyl signal (δ202.1) and appearance of an additional proton signal at δ3.75 corresponding to C-3 position in FR-008-V. The presence of a hydroxyl group at position C-3 in FR-008-V was also confirmed by the 2D-NMR spectra, in which the proton signal at δ3.75 showed correlation with a pair of germinal protons H-2 and a coupling network from H-4 to H-6 (see the Supplemental Data).

The structure of FR-008-VI differed from that of FR-008-III in the partial structure between C-3 and C-13, where the hydroxyl groups at C-9 and C-13 were absent, and an additional hydroxyl group was present at C-5 in FR-008-VI (Figure 1B). Comparison of DQF-COSY and TOCSY spectra between FR-008-VI and FR-008-III reveals that the proton signals corresponding to H-9 and H-13 of FR-008-III disappeared in FR-008-VI; instead, a novel proton signal at δ4.26 appeared in FR-008-VI, and shows correlations with two pairs of germinal proton signals at δ2.38/δ2.58 and δ2.28/δ2.33. These are all α-protons of carbonyl groups and are therefore assigned as H-5, H-4, and H-6, respectively. The structure of segment C-1 to C-6 of FR-008-VI could be confirmed by the evidence of J_{CH} long-range heteronuclear coupling correlation in the HMBC spectrum (see the Supplemental Data).

fscO Is Not Responsible for C-9 Hydroxyl Restoration

fscO, showing 34% similarity and 25% identity to an FAD-dependent monooxygenase from *Agrobacterium tumefaciens* C58, lies at the left end of the FR-008 gene cluster, and was initially assumed to restore the C-9 hydroxyl group by a tailoring modification (Chen et al., 2003). To assess the role of *fscO* in FR-008 biosynthesis, a 527 bp DNA fragment internal to *fscO* (1380 bp) was replaced by a cassette carrying the apramycin

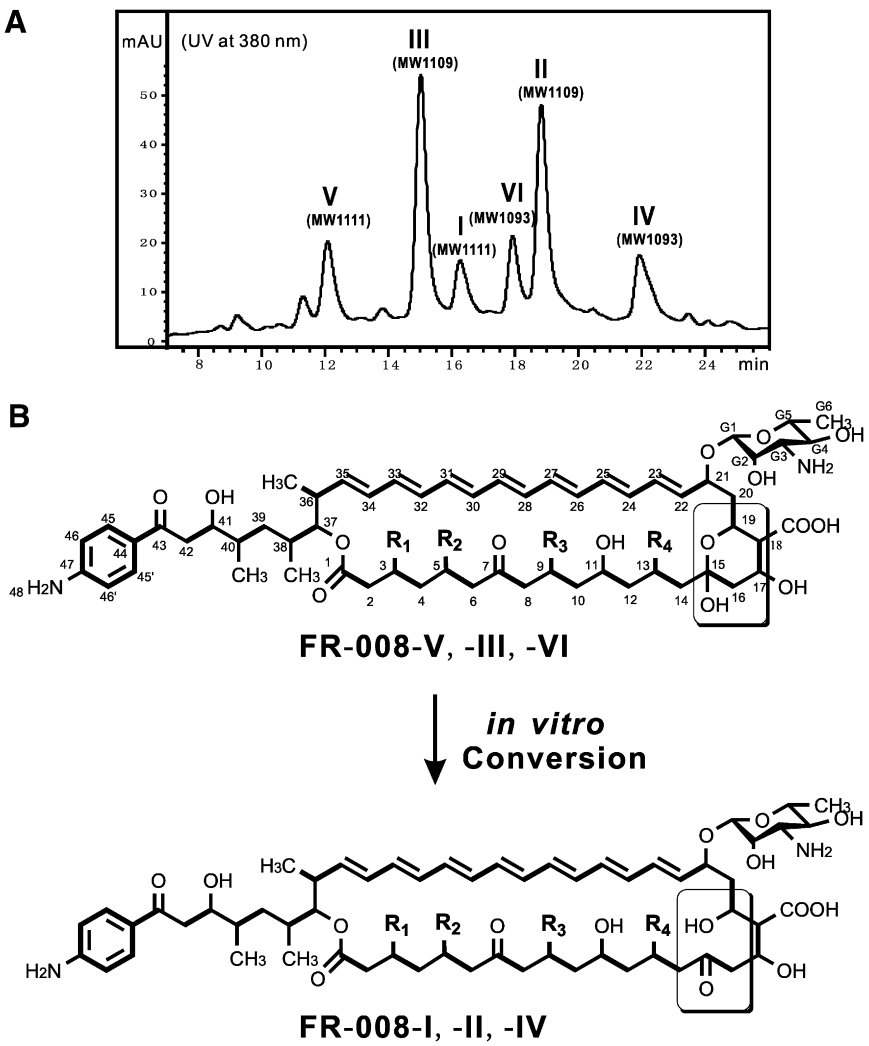

	R_1	R_2	R_3	R_4
FR-008-I, -V	OH	H	OH	OH
FR-008-II, -III	=O	H	OH	OH
FR-008-IV, -VI	=O	OH	H	H

Figure 1. LC-MS Profile and Structural Variations of Six FR-008 Components

(A) LC-MS analysis of the FR-008 sample extracted from liquid fermentation broth, or from the sample stored 1 day at room temperature after being extracted from spores or mycelia. The six components (FR-008-I to -VI) can be grouped as three pairs by identical molecular weight (MW): FR-008-I and -V (MW, 1111); FR-008-II and -III (MW, 1109); and FR-008-IV and -VI (MW, 1093).

(B) Structural variations of FR-008 components. Coexistence of ketone or hydroxyl at C-3 and also methylene or hydroxyl at C-9 in FR-008 aglycones was genetically identified as resulting from respective incomplete activities of KR21 and DH18 during polyketide biosynthesis (Figure 3). The vertical boxes highlight the hemiketal ring between C-15 and C-19 in the aglycones of FR-008-V, -III, and -VI. They also highlight the opening of the hemiketal ring in the aglycones of FR-008-I, -II, and –IV, which were respectively formed by in vitro conversions of the three former structures at room temperature. The unexpected groups at C-5 and C-13 in FR-008-VI are inconsistent with the structure predicted from domains 16 and 20 (Figure 2), and are assumed to be generated from disorder biosynthesis.

resistance gene *acc(3)IV* on the chromosome. LC/ESI-MS analysis revealed no detectable structural changes in fermentation extracts of the resultant mutant ZYJ-1 compared with that of the parental strain, and, therefore, *fscO* has no involvement in C-9 hydroxylation on FR-008 aglycone (data not shown).

Inactivation of KR21 Abolished FR-008-V Production

Structural elucidation revealed that FR-008-V and -III differed only at C-3, where a hydroxyl group in the former is replaced by a keto group in the latter (Figure 1B). According to the elongation steps of FR-008 polyketide, KR21 in FscF could reduce the β-ketothioester intermediate into the β-hydroxythioester at C-3, and, thus, should be necessary for producing FR-008-V (Figure 2). We thus set out to inactivate KR21 by generating a point mutation.

A putative catalytic triad consisting of Y (Tyr), S (Ser), and K (Lys) residues, conserved in short-chain dehydrogenases/reductases (Reid et al., 2003), was identified in KR21 based on alignment of active-site sequences of grouped KR domains from FR-008 (Figure 3A). To inactivate KR21 in FscF, the active residue Y1526 was replaced by F (Phe), with an additional restriction site (ApoI) introduced to facilitate the screening of mutants (Figure 4A). Three identical mutants of KR21 were confirmed by PCR amplification, ApoI digestion, and sequencing of the PCR products. Clearly, no FR-008-V was found to be accumulated in KR21 mutant (ZYJ-2), whereas FR-008-III and -VI were normally produced, as shown by HPLC analysis (Figure 4B). Therefore, the activity of KR21 was identified to be essential for the generation of FR-008-V bearing a C-3 hydroxyl. The total yield of FR-008/candicidin antibiotics in ZYJ-2 was approximately 60% of that from the wild-type.

Inactivation of DH18 Abolished FR-008-VI Production

DH18 and ER18 should be responsible for dehydration and enoyl reduction during the 18th elongation step, to produce

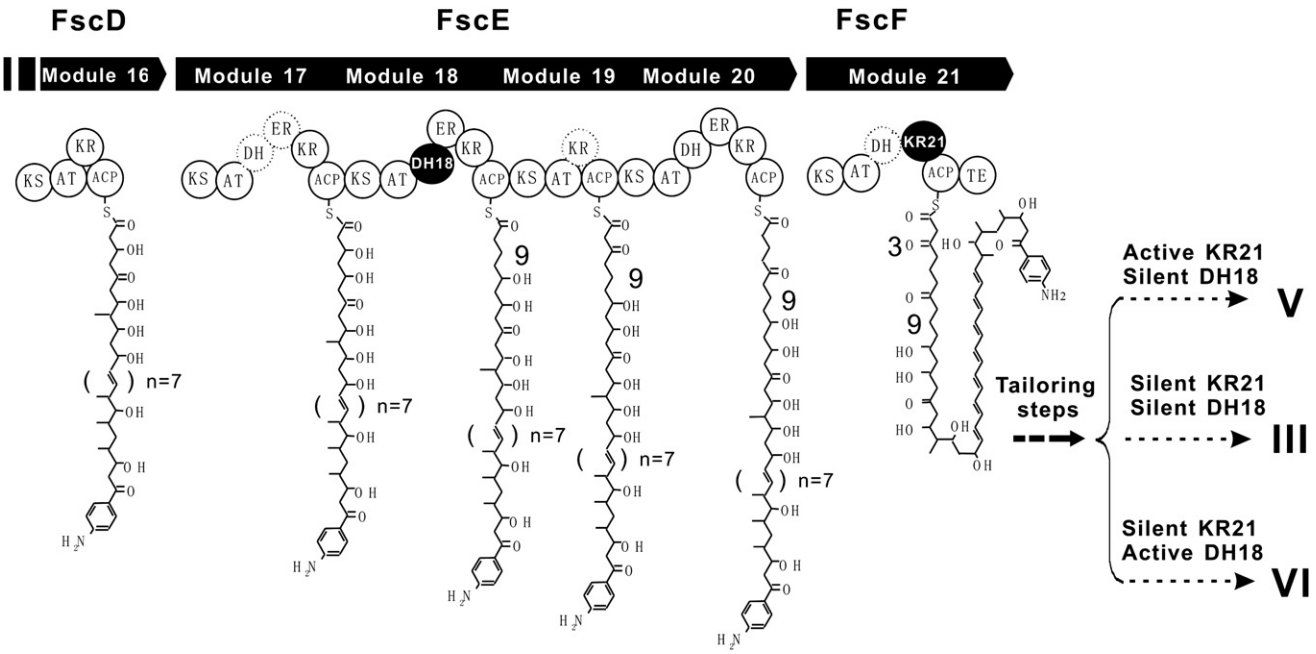

Figure 2. The 16th–21st Elongation Steps of the FR-008 Polyketide

KR21 and DH18 are marked by black circles. Dashed circles represent the silent domains. KR21 (ketoreductase) is expected to reduce C-3 β-keto into a β-hydroxyl group at the last elongation step, and DH18 (dehydratase) and ER18 (enoyl reductase) are expected to be responsible for eliminating the C-9 β-hydroxyl to generate C-9 methylene during the 18th elongation. Mutagenesis analysis of KR21 and DH18 indicated: V and III (FR-008-V and -III) were produced under the DH18 silence; III and VI (FR-008-III and -VI) were produced under the KR21 silence; and III (FR-008-III) was generated by the synchronous silences of KR21 and DH18 (Figure 4).

the C-9 methylene in the FR-008 aglycone (Figure 2). Structural characterization proved that the C-9 methylene is only present in FR-008-VI, whereas both FR-008-V and -III carry a C-9 hydroxyl instead. This implies that DH18 could have been active when forming component VI but nonfunctional when producing FR-008-V and FR-008-III (Figure 2). Keeping in mind that the activity of DH18 should be unnecessary for FR-008-V and -III production, we set out to inactivate DH18 by the means of a point mutation.

Almost all hitherto-identified DH domains from modular PKSs have the active-site motif H(X3)G(X4)P, such as the consensus sequence of DH domains in the biosynthesis of avermectin, amphotericin, rifamycin, nystatin, and nanchangmycin (Brautaset et al., 2000; Caffrey et al., 2001; Ikeda et al., 1999; Sun et al., 2003; Tang et al., 1998). The same active-site motif was found in the DHs of FR-008 (Figure 3B). The His (H) residue in the motif was suggested to be essential for catalytic activity of DH domains, since there are many cases of inactive DHs with inartificial mutation(s) at the site, such as DH17 of AmphJ and DH6 of NanA4, each with the mutation of H (His) to R (Arg) (Caffrey et al., 2001; Sun et al., 2003), and DH17 of NysJ and DH7 of AVES3, each with the mutation of H (His) to Y (Tyr) (Ikeda et al., 1999; Sun et al., 2003).

To inactivate DH18, the amino acid replacement, H3084Y in FscE, was introduced into the active site of DH18. For introducing an additional restriction site (BsrGI), D (Asp) 3083 in FscE was replaced by V (Val) simultaneously (Figure 4A) . Three identical DH18 mutants (ZYJ-3) were selected on the basis of the introduction of the additional BsrGI restriction site into the DH18 coding region.

As expected, FR-008-VI disappeared, while FR-008-V and -III accumulated normally in the fermentation extract of ZYJ-3 according to HPLC analysis (Figure 4B). DH18 is therefore confirmed to be necessary for generation of FR-008-VI by removing the C-9 hydroxyl in the FR-008 aglycone. The polyene yield of ZYJ-3 reached approximately the same level as that of the wild-type strain. Interestingly, two apparently novel components, FR-008-New-1 and -2 (Figure 4B), could be detected at relatively low levels in ZYJ-3. They were purified by preparative HPLC and subjected to LC/ESI-MS analysis, and were proven to be FR-008 analogs with typical heptaene absorption spectra, and the mass spectra, *m/z* 1108.7 $[M - H]^-$ (FR-008-New-1) and m/z 1092.6 $[M - H]^-$ (FR-008-New-2), respectively (data not show).

Only FR-008-III Preserved in KR21 and DH18 Double Mutant

Double mutant ZYJ-6 was obtained by introducing a further DH18 mutation (H3084Y and D3083V) into a pregenerated KR21 mutant, ZYJ-2, by the same way as ZYJ-3 generation in the wild-type strain (Figure 4A). The components bearing a C-3 hydroxyl (FR-008-V) or a C-9 methylene (FR-008-VI) were destroyed, and only FR-008-III produced under the nonfunctional DH18 and KR21 was preserved in the resultant mutant ZYJ-6 (Figure 4B). The polyene yield in ZYJ-6 was approximately 80% of the wild-type level. Interestingly, FR-008-New-1 and -2 were also accumulated in ZYJ-6 (Figure 4B).

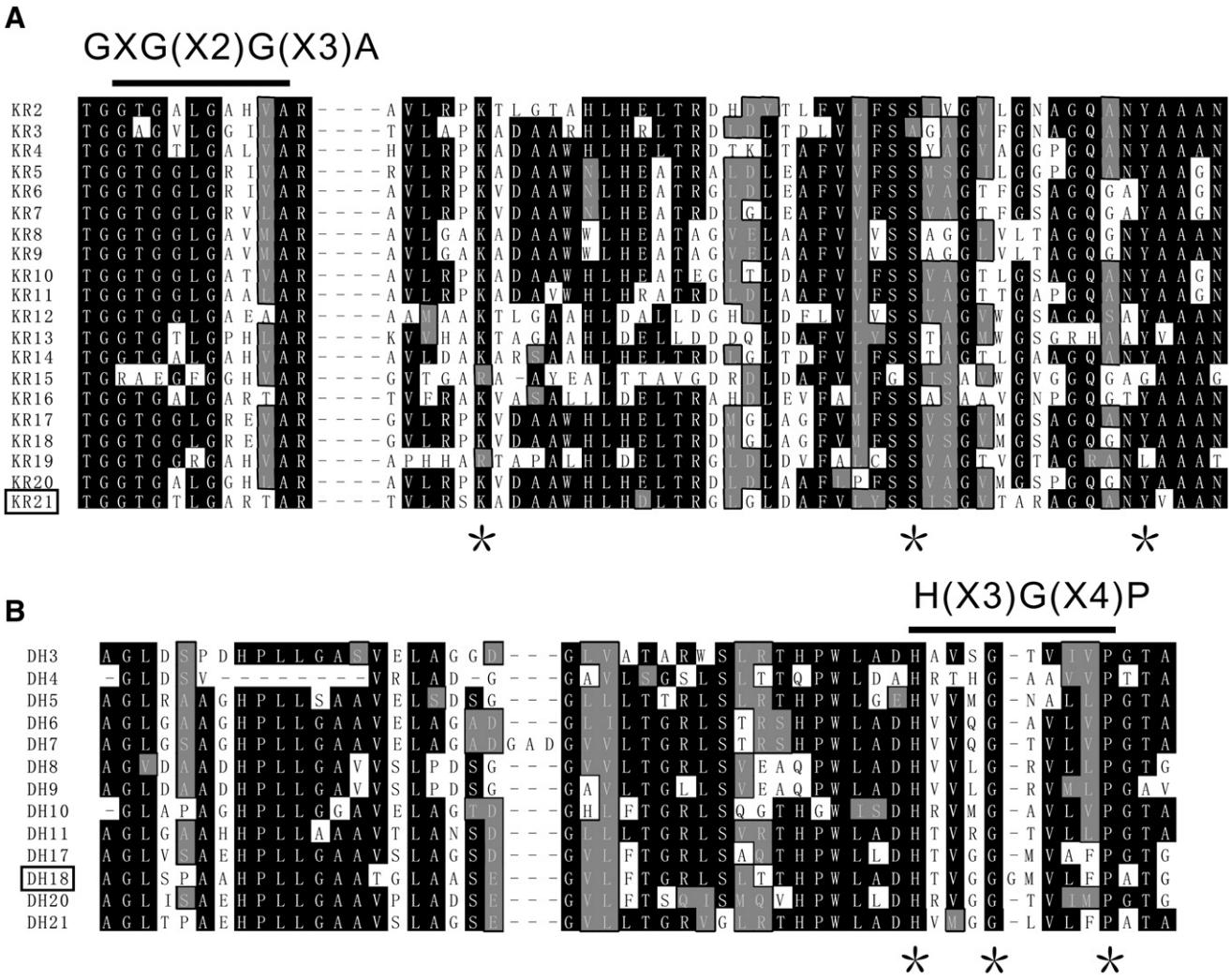

Figure 3. Alignment of Active-Site Sequences of Grouped KR Domains and DH Domains from FR-008 PKSs

Only the regions containing proposed active sites are shown. The proposed catalytic residues are marked with asterisks. (A) KR domains and (B) DH domains (KR21 and DH18 discussed in this work are boxed). Solid bars represent the conserved motifs, GXG(X2)G(X3)A as NADP(H) binding motif in KRs; H(X3)G(X4)P as active-site motif in DHs.

Comparison of the Antifungal Activities of FR-008-V, -III, and -VI

A series of 2-fold antibiotic dilutions were tested for growth inhibition of the test organism, *S. cerevisiae* Y029 (see the Experimental Procedures). GI_{50} values (50% of isolates inhibited) were estimated from the inhibition curve of each polyene. The antifungal activity of FR-008-III (0.90 μg/ml) was about twice that of FR-008-V (2.0 μg/ml), and comparable to that of FR-008-VI (0.75 μg/ml).

DISCUSSION

While the FR-008/candicidin complex produced from either *S. griesus* IMRU3570 or *Streptomyces* sp. FR-008 was previously reported to be biosynthesized as a mixture of four derivatives (i.e., candicidin A, B, C, and D, or FR-008-I, -II, -III, and -IV [Chen et al., 2003; Zielinski et al., 1979]), our recent analysis using improved LC-MS actually detected six FR-008 components (FR-008-I to VI) coexisting in the fermentation broth extract (Figure 1A), which can be grouped as two additional pairs of isomers by their identical MS spectra (i.e., FR-008-I and -V, and -IV and -VI, apart from the previously assumed isomeric pair of FR-008-II and III [Chen et al., 2003]). The structure characterization of FR-008-II and -III supports the interpretation of FR-008-III being an isomer of FR-008-II, due to hemiketal moiety formation between C-15 and C-19, and two other pairs of components (i.e., FR-008-I and -V, and -IV and -VI) may have derived in a similar way. Further work indicated that only FR-008-V, -III, and -VI were present in the fresh sample extracted from cells, and the counterpart isomers FR-008-I, -II, and -IV were produced in vitro during the prolonged storage (Figure 1B). The hemiketal ring, therefore, should have been formed between the hydroxyl of C-19 and the keto of C-15 in FR-008 precursor before release, and FR-008-III, -V, and -VI should only be

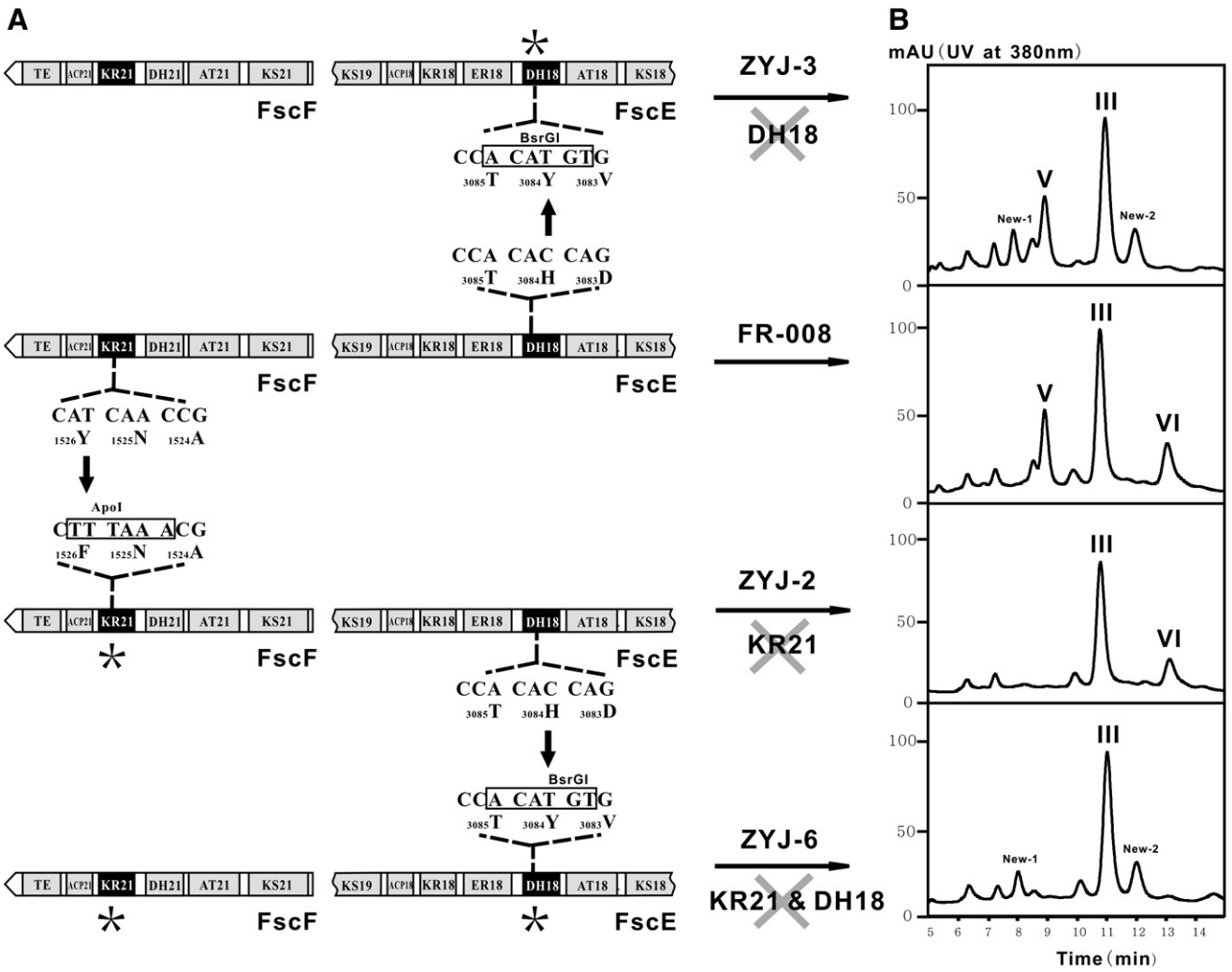

Figure 4. The Activities of KR21 and DH18 Related to Coproduction of Three Main FR-008 Components

(A) Mutation sites in DH18 and KR21 domains, and the relationship between the wild-type (FR-008) and its mutants (ZYJ-2, -3, and -6). Asterisks represent the mutated domains. The mutation in KR21 is Y1526F with an additional restriction site (ApoI) introduced. The mutation in DH18 is H3084Y with an additional mutation, D3083V, generated for introducing a restriction site (BsrGI).

(B) HPLC analysis (detection at 380 nm) of the fermentation culture extracts of ZYJ-2, -3, and -6 compared with wild-type. Three major FR-008 components (V, III, and VI) were detected in the wild-type, while component V was absent in ZYJ-2; ZYJ-3 lost production of VI; and the double mutant (ZYJ-6) produced only III. Two novel components (FR-008-New-1 and -2) detected in ZYJ-3 and -6 are marked as New-1 and New-2, respectively.

regarded as the authentic natural products that resulted from FR-008 biosynthesis.

Indeed, the retention of the C-3 keto group in FR-008-III and -VI, and of the C-9 hydroxyl in FR-008-III and -V (Figure 1B), would disagree with the characterized biosynthetic pathway mostly based on bioinformatic alignments if KR21 (which reduces the β-keto into a β-hydroxyl group at C-3 of the FR-008 aglycone during the final elongation step) and DH18-ER18 (which reduces the β-carbon atom during the 18th elongation step at the C-9 position) could exert their full activities (Figure 2). Our knockout experiments targeting the specific residues of DH18 and KR21 supported the hypothesis that they could not fully execute their activities during polyketide elongation. Furthermore, in view of the capacity of some reported P450 monooxygenases to introduce a hydroxyl group at the polyol region of polyene aglycone during the tailoring modification step (Byrne et al., 2003; Volokhan et al., 2006), the possibility that some unidentified tailoring modification(s) existed for C-9 hydroxylation in FR-008 aglycone could not be ruled out completely. It is worth mentioning, however, that neither *fscO* (FAD-dependent monooxygenase) nor *fscP* (P450 monooxygenase gene) from the FR-008 gene cluster would be responsible for the restoration of the C-9 hydroxyl based on knockout experiments (S. Chen et al., unpublished data about *fscP*).

KR21 and DH18 seem to be only about 21% and 23% active, respectively, as a result of an estimated production ratio (2.6:1.0:1.1 for FR-008-III:-V:-VI) derived from by HPLC analysis. The generated KR21 and DH18 double mutant could have resulted in a complete silencing of the KR21 and DH18 activity, as FR-008-III was principally accumulated, although at only

slightly increased levels as compared with that yielded from the wild-type producer.

The sluggish activity of KR21 should not attribute to its inefficient utilization of NADP(H), since there are no abnormal alterations found in the NADP(H) binding motif (Aparicio et al., 1996; Scrutton et al., 1990; Tang et al., 1998) of KR21 (Figure 3A). The seemingly constant production ratio of the FR-008 series of compounds, while adjusting NADP(H) supplies by changing glucose concentrations in the fermentation medium, also agrees with this assumption (data not shown). This is especially so, when one considers that NADPH is produced in bacteria mainly through the pentose phosphate pathway (Borgos et al., 2006).

A seemingly redundant residue (G3089 in FscE) in the DH18 active-site motif H(X3)GG(X4)P compared to the normal H(X3)G(X4)P in DHs could not be argued, at present, as a cause for incomplete activity of DH18. This is because the DH3 in amphotericin biosynthesis carrying the mismatched active-site motif (H(X3)A(X4)P) (Caffrey et al., 2001) functions well, and the DH2 in AVES1 was unable to restore the full activity by the normal substitution of the mismatched active-site motif (H(X3)G(X4)S) (Ikeda et al., 1999). We have not tried to investigate this question by replacing the native active-site motif with the normal one.

Similar to the unexplained incomplete activity of KR21, many intact DH domains were unreasonably silent in PKSs with intact conserved consensus sequence, such as DH17 and DH21 in FR-008, DH15 in AmphJ, DH18 in NysK, and DH6 and DH7 in the rifamycin PKS (Brautaset et al., 2000; Caffrey et al., 2001; Chen et al., 2003; Tang et al., 1998). It can reasonably be stated that, except for the active-site motif, the activities of catalytic domains in multifunctional PKS proteins may also be affected by the interdomain sequences, and even by overall protein conformations, such as the sluggish activity of ER5 in AmphC presumed to be attributable to a shortened interdomain preceding ER5, which may restrict movement of the ER5 (Caffrey et al., 2001). Many engineered hybrid PKS proteins cannot reach ideal catalytic efficiencies, likely because of the disturbance to native PKS protein conformations (Kim et al., 2004; McDaniel et al., 1997; Menzella et al., 2005). One plausible explanation for incomplete action of KR21 may be that the TE domain (Gokhale et al., 1999) at the C terminus of FscF could not sufficiently distinguish between the oxidized form of the polyketide and the form reduced by KR21 prior to cyclization and release (Chen et al., 2003). The incomplete action of DH18 may reflect the premature transfer of the chain from ACP18 to KS19 before DH18 could complete its function.

An unexpected absence of a hydroxyl at C-13 and its unexpected presence at C-5 in FR-008-VI (Figure 1B) is somewhat confusing, as the positional swapping of this hydroxyl group is totally unexpected from the detected structures of FR-008-V and -III well consistent with the deduced biosynthesis pathway, in which the C-13 hydroxyl group should be preserved because module 16 lacks DH-ER domains, and the C-5 methylene should be logically generated by the presence of functional DH20-ER20 (Figure 2). The generation of FR-008-VI may represented an ''out-of-order'' catalysis related to a certain conformation of FscE, in which the DH18-ER18 may not only act to reduce the C-9 hydroxyl group specifically, but also exert its duty to the C-13 hydroxyl group derived from upstream 16th elongation, and thus gave fully reduced C-9 and C-13 atoms, while the silent DH20 in the case permitted reservation of C-5 hydroxyl. Offloaded from FscE, the FR-008-VI precursor processed in FscF may not be the proper substrate of KR21 for β-ketone reduction at C-3 position, and thus the FR-008-VI aglycone was produced. Obviously, the hypothesis needs to be supported experimentally (e.g., by generating further mutations and/or PKS protein structure elucidations). Noticeably, another likely atypical PKS was also found in epothilones biosynthesis, in which the lack of dehydratase domain in module 4 disagrees with the double bond formation at C12-13 in epothilones structure (Tang et al., 2000).

Trace amounts of two FR-008 compounds (FR-008-New-1 and -2) appeared in the fermentation extract of the DH18 mutants (ZYJ-3 and ZYJ-6) (Figure 4B). Obviously, the generation of these compounds depends on DH18 mutation, which may have influenced or altered the activities or specificities of other catalytic domains in FscE.

Clearly, elucidating the factors controlling metabolite distributions so as to accumulate more desirable components by rational manipulation of the biosynthetic pathways would be of great value for drug discovery and/or strain improvement. Thus, there is evident value in our present work, which is based on the detailed elucidation of the molecular structures of three major FR-008 components (FR-008-III, -V, and -VI), genetically coproduced largely as a result of incomplete activities of KR21 and DH18. In addition, the use of the information for the creation of a mutant strain producing only one of the superior antifungal components (FR-008-III) at considerable yield is an additional example of the potential of metabolic engineering employing antibiotic producers.

SIGNIFICANCE

Glycosylated polyenes represent a major and very complex class of antifungal agents, within which candicidin appeared as the earliest model complex of this family. Considerable progress had been made in research into this complex, but little has yet been elucidated about the mechanisms, especially the genetic controls, of their structural variations. Our efforts for the detailed characterization of the candicidin complex compounds not only enabled us to distinguish the compounds resulting from in vivo conversions, but also the in vitro process, leading to the studies on the intrinsic mechanism of the in vivo conversions. This opened a window for the creation of more structural variations, or generation of strains with predominant production of a unique desirable compound by the rational manipulation of a specific domain or a combination of specific domains. This may help in the creation of polyene derivatives with improved pharmacological properties, increased activity, reduced toxicity, or improved water solubility.

EXPERIMENTAL PROCEDURES

Bacterial Strains, Plasmids, Culture Techniques, and General Techniques

Streptomyces sp. FR-008 (Chen et al., 2003), the wild-type producer of antibiotic FR-008, was used for antibiotic isolation and generation of mutant strains by targeted gene disruption and replacement. The bioassay organism was *S. cerevisiae* Y029, grown in YEME medium at 30°C. DH5α (F$^-$, *rec*A, *lac*Z,

ΔM15) (Hanahan and Meselson, 1983) was used as *E. coli* host. pHZ1358 (Sun et al., 2002) (an *E. coli* and *Streptomyces* shuttle vector) was used for gene replacement. pBluescript II SK(+) (Short et al., 1988), pIJ2925 (Janssen and Bibb, 1993) and PMD 18-T vector (TaKaRa) were used for clone construction or DNA sequencing. SFM medium (2% agar, 2% mannitol, 2% soybean powder [pH 7.2~7.5]) was used for sporulation (30°C, 3 days), solid fermentation (30°C, 6 days), and conjugation. YEME medium was used for liquid fermentation (30°C, 2 days), and TSBY medium (10.3% sucrose) was used for growth of mycelium and isolation of total DNA. LB medium was used for *E. coli* propagation. Recombinant DNA techniques were described by Sambrook et al. (1989). PCR reactions were performed with KOD-Plus (TOYOBO).

Bioassay

The concentrations of antibiotics were calculated by measuring the area of UV peaks at 380 nm in HPLC analysis. Series of 2-fold antibiotic dilutions in DMSO were prepared for determining the concentrations yielded from complete growth inhibition to no growth inhibition of the test organism. Test organism cultures mixed with antibiotic dilutions were incubated at 30°C with shaking at 220 rpm for 8 hr. The optical density measured at 540 nm was plotted against the antibiotic concentrations to produce a standard inhibition curve. GI_{50} (50% of isolates inhibited) was estimated from the repression curve and used for comparing the activities of each polyene.

Polyene Extraction and Preparative Purification

Wild-type and mutants of *Streptomyces* sp. FR-008 were grown on SFM at 30°C for 8 days. Solid fermentation cultures were extracted with 2 volumes of methanol three times. The extract solvent was filtrated and concentrated by evaporation, and then adjusted to 20% methanol solvent, and applied to a column of C-18 ODS (Kromasil). After washing the column with 2 volumes of 20% and 40% methanol, in turn, the active fraction was eluted with 100% methanol, and subsequently evaporated to dryness. The sample was then dissolved in a small amount of DMSO ready for subjecting to preparative reverse-phase HPLC (Shimadzu) on a Shimadzu C_{18} 20 × 250 mm column at a flow rate of 8 ml/min. The mobile phase was 45% acetone in 5.5 mmol ammonium acetate (pH 4.5). Each compound was purified by preparative HPLC twice. The relevant collected fractions were quickly evaporated to aqueous residues at 45°C in darkness, and then adjusted to 10% acetone solvent for application to a 5 cm LC-C18 column (Merck) for sample enrichment and removal of salt. After washing with 10% methanol, the final sample was eluted with a small volume of 100% methanol and then dried to a yellow powder under freezing vacuum. The purity of each sample was above 95%, as assessed by LC-MS analysis.

LC-MS Analysis of Polyene Samples

Polyene samples were extracted with methanol from spores harvested after 6 day cultivation on soybean agar. LC-MS was operated with the Agilent 1100 series LC/MSD Trap system. The LC column was an Agilent Eclipse XDB-C18, with dimensions 4.6 × 250 mm run at a flow rate of 0.6 ml min^{-1}, and the mobile phase was 45% CH_3CN in 5.5 mmol ammonium acetate (pH 4.5). The ion trap mass spectrometer was operated with the electrospray ionization source in the negative or positive ion mode. Drying gas flow was 10 l/min, and nebulizer pressure was 50 psi. Drying gas temperature was 350°C. The fragmentation amplitude was varied between 1.0 and 1.8 V.

NMR Experiments

The sample of FR-008 components was dissolved in 500 μl of DMSO-d_6, and TMS was used as internal reference. All NMR experiments were carried out at 600 MHz and 25°C on a Unity Inova600 Spectrometer. Two-dimensional spectra, such as DQF-COSY (Derome and Willamson, 1990), TOCSY (Bax and Davis, 1985), and rotating frame nuclear Overhauser effect spectroscopy (Jeener et al., 1979) were performed in phase-sensitive mode by a time-proportional phase incrementation method. 2D-^{1}H-NMR spectra were recorded with 2,000 (4,000 for DQF-COSY) data points in the t_2 dimension, and 512 points in the t_1 dimension in the hypercomplex mode. Raw data were weighted with a phase-shifted, squared sine bell window function, zero-filled and Fourier-transformed to obtain a final matrix of 4,000 × 4,000 data points. The TOCSY spectra were acquired with the MLEV-17 pulse, with a mixing time of 80 ms. The ROESY spectra were measured with a mixing time of 400 ms. Chemical shifts were calibrated with TMS.

Knockout *fscO* Gene

A 9.0-kb BamHI fragment isolated from pHZ145 (Hu et al., 1994) was cloned into the BamHI site of pBluescript SK^+ to give pJTU553, which embodies two fragments (2.7 kb *Not*I-KpnI and 2.5 kb SmaI-BamHI) localized beside the region, nt 1188–660 bp downstream of the start codon of *fscO* (1380 bp). One cassette (1.4 kb EcoRI-SmaI fragment) carrying the apramycin resistance gene, *acc(3)IV*, was sandwiched between the two fragments recovered from pJTU553 on the vector pIJ2925, to give pJTU559. The 6.6 kb recombinant fragment with the internal *acc(3)IV* gene was BamHI-digested from pJTU559 for ligation into the BamHI site of pHZ1358 to generate a final construction of pJTU563, which was transferred by conjugation from *E. coli* ET12567 carrying the RP4 derivative pUZ8002 (Mazodier et al., 1989) into *Streptomyces* sp. FR-008. Thiostrepton-sensitive and apramycin-resistant ($Thio^S$-Apr^R) colonies were counterselected from the initial $Thio^R$-Apr^R exconjugants after two rounds of nonselective growth. Three selected $Thio^S$-Apr^R exconjugants were identified as desired mutants by PCR with primers fscOL 5′-TTGTTCTGCTCCTGCCACCA-3′ (sense) and fscOR 5′-AACGCTTCGA CCTGGTCATA-3′ (antisense). The 1650 bp PCR product was amplified from the mutant compared with a 732 bp PCR product from the wild-type. Sequencing the 1650 bp PCR product gave further confirmation of the resultant mutant ZYJ-1.

Point Mutation of KR21: ZYJ-2

For introducing the mutation Y1526F into the active motif of the KR21 domain (Figure 4A) by targeted gene replacement, the following two pairs of primers were used: P1, 5′-CCGCCTCACCCAACTGCC-3′ (sense) and P3, 5′-GCGACG AAATTTGCCTGGCCG-3′ (antisense); P4, 5′-CCA GGCAAATTTCGTCGC CGC-3′ (sense) and P2, 5′-GGGGAG CCGCTGTCGTAGA-3′(antisense) (the introduced restriction site [ApoI] is underlined; P1 and P3 were used for amplifying 528 bp; P4 and P2 were used for amplifying 618 bp). The two PCR fragments with 18 bp end-to-end overlapping were then used as template for amplifying a 1146 bp fragment with the primers P1 and P2. The 1146 bp PCR product was digested into one 849 bp SacI-SfiI fragment, and used for replacing the corresponding region of the 3615 bp EcoRI-KpnI fragment, which was recovered from cosmid pHZ220 (Hu et al., 1994) and cloned into EcoRI- and KpnI-digested pIJ2925. The recombinant 3615 bp fragment was then excised as a BglII-BglII fragment and cloned into the unique BamHI site of pHZ1358 (Sun et al., 2002) to create pJTU573, which was introduced into strain FR-008 by conjugation from the nonmethylating *E. coli* donor strain ET12567::pUZ8002 (Mazodier et al., 1989). $Thio^S$ colonies were counterselected from the initial $Thio^R$ exconjugants after two rounds of nonselective growth and used as mutant candidates tested by PCR with primer pairs P1 and P2, and ApoI digestion. The 1146 bp PCR product from the resultant mutant (ZYJ-2) could be digested into 528 bp and 618 bp by ApoI. The PCR fragment was also introduced into T vector (TaKaRa) for sequencing as further confirmation of the desired mutation.

Point Mutation of DH18: ZYJ-3

To engineer the construction for introducing the mutation of H3084Y and D3083V in the active motif of the DH18 domain (Figure 4A), 1475 and 1203 bp fragments were amplified, respectively, with the primers: DH18P1, 5′-GAC ACGGAGTCCCCCGAGCCCCAGG-3′ (sense); DH18P2, 5′-CCG ACGGTGTA CACGGCGAGCCAGG−3′ (antisense); and DH18P3, 5′-CCTGGCTCGCCG TGTACACCGTCGG-3′ (sense); DH18P4, 5′-CGCCCGAGAGCGGACCGAGG AGTTG-3′ (antisense) (the introduced restriction site [BsrGI] is underlined). The two fragments were respectively cloned into transitional vectors (pBluescript II SK(+) and T-Vector) and sequenced, and then joined to a 2678 bp fragment by the introduced BsrGI site. The 2678 bp fragment was then excised and inserted into the BamHI site of pHZ1358 to generate plasmid pJTU572, used as final construct for point mutation of DH18 by the same procedures as that for the KR21 mutation. The desired mutation in the resultant mutant strain (ZYJ-3) was tested by BsrGI digestion of the PCR product with primers DH-test-L (5′-GCTCTACCGTCCGCTTCGCC-3′) and DH-test-R (5′-CTGTGT CCAGGTGGCGTCCG-3′). The 706 bp PCR product amplified from the mutant

should be digested into 244 and 462 bp by BsrGI, and the PCR product was sequenced as further proof of the desired mutation.

Double Mutations of KR21 and DH18: ZYJ-6

For obtaining double mutation of KR21 and DH18, pJTU572 was also transferred into the KR21 mutant (ZYJ-2) by conjugation with the same procedures as that described above. The double mutation (ZYJ-6) was screened and confirmed by the same strategy as that used for ZYJ-2 and ZYJ-3.

SUPPLEMENTAL DATA

Supplemental Data include Supplemental Results and Supplemental Experimental Procedures used in this work, and one table and are available online at http://www.chembiol.com/cgi/content/full/15/6/629/DC1/.

ACKNOWLEDGMENTS

We are very grateful to Sir David Hopwood, FRS, for critical and patient editing of the manuscript. We also thank the National Science Foundation of China, the Ministry of Science and Technology (programs 973 and 863), and the Shanghai Municipal Council of Science and Technology for research support.

Received: February 18, 2008
Revised: April 29, 2008
Accepted: May 6, 2008
Published: June 20, 2008

REFERENCES

Aparicio, J.F., Molnar, I., Schwecke, T., Konig, A., Haydock, S.F., Khaw, L.E., Staunton, J., and Leadlay, P.F. (1996). Organization of the biosynthetic gene cluster for rapamycin in *Streptomyces hygroscopicus*: analysis of the enzymatic domains in the modular polyketide synthase. Gene *169*, 9–16.

Aparicio, J.F., Fouces, R., Mendes, M.V., Olivera, N., and Martin, J.F. (2000). A complex multienzyme system encoded by five polyketide synthase genes is involved in the biosynthesis of the 26-membered polyene macrolide pimaricin in *Streptomyces natalensis*. Chem. Biol. *7*, 895–905.

Aparicio, J.F., Caffrey, P., Gil, J.A., and Zotchev, S.B. (2003). Polyene antibiotic biosynthesis gene clusters. Appl. Microbiol. Biotechnol. *61*, 179–188.

Bax, A., and Davis, D.G. (1985). MLEV-17-based two-dimensional homonuclear magnetization transfer spectroscopy. J. Magn. Reson. *65*, 355–360.

Bolard, J. (1986). How do the polyene macrolide antibiotics affect the cellular membrane properties? Biochim. Biophys. Acta *864*, 257–304.

Borgos, S.E., Sletta, H., Fjaervik, E., Brautaset, T., Ellingsen, T.E., Gulliksen, O.M., and Zotchev, S.B. (2006). Effect of glucose limitation and specific mutations in the module 5 enoyl reductase domains in the nystatin and amphotericin polyketide synthases on polyene macrolide biosynthesis. Arch. Microbiol. *185*, 165–171.

Brautaset, T., Sekurova, O.N., Sletta, H., Ellingsen, T.E., StrLm, A.R., Valla, S., and Zotchev, S.B. (2000). Biosynthesis of the polyene antifungal antibiotic nystatin in *Streptomyces noursei* ATCC 11455: analysis of the gene cluster and deduction of the biosynthetic pathway. Chem. Biol. *7*, 395–403.

Bruheim, P., Borgos, S.E., Tsan, P., Sletta, H., Ellingsen, T.E., Lancelin, J.M., and Zotchev, S.B. (2004). Chemical diversity of polyene macrolides produced by *Streptomyces noursei* ATCC 11455 and recombinant strain ERD44 with genetically altered polyketide synthase NysC. Antimicrob. Agents Chemother. *48*, 4120–4129.

Byrne, B., Carmody, M., Gibson, E., Rawlings, B., and Caffrey, P. (2003). Biosynthesis of deoxyamphotericins and deoxyamphoteronolides by engineered strains of *Streptomyces nodosus*. Chem. Biol. *10*, 1215–1224.

Caffrey, P., Lynch, S., Flood, E., Finnan, S., and Oliynyk, M. (2001). Amphotericin biosynthesis in *Streptomyces nodosus*: deductions from analysis of polyketide synthase and late genes. Chem. Biol. *8*, 713–723.

Campelo, A.B., and Gil, J.A. (2002). The candicidin gene cluster from *Streptomyces griseus* IMRU 3570. Microbiology *148*, 51–59.

Chen, S., Huang, X., Zhou, X., Bai, L., He, J., Jeong, K.J., Lee, S.Y., and Deng, Z. (2003). Organizational and mutational analysis of a complete FR-008/candicidin gene cluster encoding a structurally related polyene complex. Chem. Biol. *10*, 1065–1076.

Derome, A., and Willamson, M. (1990). Rapid pulsing in double-quantum-filtered COSY. J. Magn. Reson. *88*, 177–185.

Gokhale, R.S., Hunziker, D., Cane, D.E., and Khosla, C. (1999). Mechanism and specificity of the terminal thioesterase domain from the erythromycin polyketide synthase. Chem. Biol. *6*, 117–125.

Hanahan, D., and Meselson, M. (1983). Plasmid screening at high colony density. Methods Enzymol. *100*, 333–342.

Hopwood, D.A., and Sherman, D.H. (1990). Molecular genetics of polyketides and its comparison to fatty acid biosynthesis. Annu. Rev. Genet. *24*, 37–66.

Hu, Z., Bao, K., Zhou, X., Zhou, Q., Hopwood, D.A., Kieser, T., and Deng, Z. (1994). Repeated polyketide synthase modules involved in the biosynthesis of a heptaene macrolide by *Streptomyces* sp. FR-008. Mol. Microbiol. *14*, 163–172.

Ikeda, H., Nonomiya, T., Usami, M., Ohta, T., and Omura, S. (1999). Organization of the biosynthetic gene cluster for the polyketide anthelmintic macrolide avermectin in *Streptomyces avermitilis*. Proc. Natl. Acad. Sci. U.S.A. *96*, 9509–9514.

Janssen, G.R., and Bibb, M.J. (1993). Derivatives of pUC18 that have BglII sites flanking a modified multiple cloning site and that retain the ability to identify recombinant clones by visual screening of *Escherichia coli* colonies. Gene *124*, 133–134.

Jeener, J., Meier, B.H., Bachmann, P., and Ernst, R.R. (1979). Investigation of exchange process by two-dimensional NMR spectroiscopy. J. Chem. Phys. *71*, 4546–4553.

Katz, L., and Donadio, S. (1993). Polyketide synthesis: prospects for hybrid antibiotics. Annu. Rev. Microbiol. *47*, 875–912.

Kim, C.Y., Alekseyev, V.Y., Chen, A.Y., Tang, Y., Cane, D.E., and Khosla, C. (2004). Reconstituting modular activity from separated domains of 6-deoxyerythronolide B synthase. Biochemistry *43*, 13892–13898.

Marsden, A.F., Wilkinson, B., Cortes, J., Dunster, N.J., Staunton, J., and Leadlay, P.F. (1998). Engineering broader specificity into an antibiotic-producing polyketide synthase. Science *279*, 199–202.

Mazodier, P., Petter, R., and Thompson, C. (1989). Intergeneric conjugation between *Escherichia coli* and *Streptomyces* species. J. Bacteriol. *171*, 3583–3585.

McDaniel, R., Kao, C.M., Hwang, S.J., and Khosla, C. (1997). Engineered intermodular and intramodular polyketide synthase fusions. Chem. Biol. *4*, 667–674.

Menzella, H.G., Reid, R., Carney, J.R., Chandran, S.S., Reisinger, S.J., Patel, K.G., Hopwood, D.A., and Santi, D.V. (2005). Combinatorial polyketide biosynthesis by de novo design and rearrangement of modular polyketide synthase genes. Nat. Biotechnol. *23*, 1171–1176.

Reid, R., Piagentini, M., Rodriguez, E., Ashley, G., Viswanathan, N., Carney, J., Santi, D.V., Hutchinson, C.R., and McDaniel, R. (2003). A model of structure and catalysis for ketoreductase domains in modular polyketide synthases. Biochemistry *42*, 72–79.

Sambrook, J., Fritsch, E.F., and Maniatis, T. (1989). Molecular Cloning: A Laboratory Manual, Second Edition (Cold Spring Harbor, NY: Cold Spring Harbor Laboratory Press).

Schwecke, T., Aparicio, J.F., Molnar, I., Konig, A., Khaw, L.E., Haydock, S.F., Oliynyk, M., Caffrey, P., Cortes, J., Lester, J.B., et al. (1995). The biosynthetic gene cluster for the polyketide immunosuppressant rapamycin. Proc. Natl. Acad. Sci. U.S.A. *92*, 7839–7843.

Scrutton, N.S., Berry, A., and Perham, R.N. (1990). Redesign of the coenzyme specificity of a dehydrogenase by protein engineering. Nature *343*, 38–43.

Short, J.M., Fernandez, J.M., Sorge, J.A., and Huse, W.D. (1988). Lambda ZAP: a bacteriophage lambda expression vector with in vivo excision properties. Nucleic Acids Res. *16*, 7583–7600.

Stassi, D., Post, D., Satter, M., Jackson, M., and Maine, G. (1998). A genetically engineered strain of *Saccharopolyspora erythraea* that produces

6,12-dideoxyerythromycin A as the major fermentation product. Appl. Microbiol. Biotechnol. *49*, 725–731.

Stutzman-Engwall, K., Conlon, S., Fedechko, R., McArthur, H., Pekrun, K., Chen, Y., Jenne, S., La, C., Trinh, N., Kim, S., et al. (2005). Semi-synthetic DNA shuffling of *aveC* leads to improved industrial scale production of doramectin by *Streptomyces avermitilis*. Metab. Eng. *7*, 27–37.

Sun, Y., Zhou, X., Liu, J., Bao, K., Zhang, G., Tu, G., Kieser, T., and Deng, Z. (2002). '*Streptomyces nanchangensis*', a producer of the insecticidal polyether antibiotic nanchangmycin and the antiparasitic macrolide meilingmycin, contains multiple polyketide gene clusters. Microbiology *148*, 361–371.

Sun, Y., Zhou, X., Dong, H., Tu, G., Wang, M., Wang, B., and Deng, Z. (2003). A complete gene cluster from *Streptomyces nanchangensis* NS3226 encoding biosynthesis of the polyether ionophore nanchangmycin. Chem. Biol. *10*, 431–441.

Tang, L., Yoon, Y.J., Choi, C.Y., and Hutchinson, C.R. (1998). Characterization of the enzymatic domains in the modular polyketide synthase involved in rifamycin B biosynthesis by *Amycolatopsis mediterranei*. Gene *216*, 255–265.

Tang, L., Shah, S., Chung, L., Carney, J., Katz, L., Khosla, C., and Julien, B. (2000). Cloning and heterologous expression of the epothilone gene cluster. Science *287*, 640–642.

Volokhan, O., Sletta, H., Ellingsen, T.E., and Zotchev, S.B. (2006). Characterization of the P450 monooxygenase NysL, responsible for C-10 hydroxylation during biosynthesis of the polyene macrolide antibiotic nystatin in *Streptomyces noursei*. Appl. Environ. Microbiol. *72*, 2514–2519.

Xue, Y., and Sherman, D.H. (2000). Alternative modular polyketide synthase expression controls macrolactone structure. Nature *403*, 571–575.

Zielinski, J., Borowy-Borowski, H., Golik, J., Gumieniak, J., Ziminski, T., Kolodzi-Ejczyk, P., Pawlak, J., and Borowski, E. (1979). The structure of levorin A_2 and candicidin D. Tetrahedron Lett. *20*, 1791–1794.

Zotchev, S.B. (2003). Polyene macrolide antibiotics and their applications in human therapy. Curr. Med. Chem. *10*, 211–223.

